Thermal management in GaN-devices for increased power density

Mohamadali Malakoutian[1], Xiang Zheng[3], Martin Kuball[3], and Srabanti Chowdhury[1,2]

[1]Department of Electrical Engineering, Stanford University, Stanford, CA, USA
[2]Department of Materials Science and Engineering, Stanford University, Stanford, CA, USA
[3]Center for Device Thermography and Reliability, University of Bristol, Bristol BS8 1TL, U.K.
E-mail: srabanti@stanford.edu

Keywords: Diamond-Integration, Thermal-Management, GaN, Low-Temperature, All-Around, Heat-Spreading

Abstract

The increasing demand for higher power density is a major trend for almost all electronic applications spanning from power to RF electronics. Gallium Nitride HEMT technology is a frontrunner in both power and RF application, due to its remarkable material properties that offer high-frequency operation simultaneously with higher power. However, we are still far from experiencing the full potential of GaN HEMT in power densities, for which thermal management is necessary. At the desired power densities, GaN HEMTs suffer from severe Joule heating that results in performance degradation and premature failure. A potential solution for increasing the efficiency in GaN HEMTs has been recognized in its integration with diamond, known for its excellent thermal properties. GaN-on-Diamond has been an attractive area of research, that was surveyed under major programs like DARPA ICECool and NJTT. On the other hand, diamond growth on GaN, although explored, did not have much success due to difficulties with diamond-centric processing. Recently our group has demonstrated several key results suitable for Diamond-on-GaN integration. Our integration technique has demonstrated the growth of diamond films at low temperature (down to 400°C) **near the hot spot in the GaN channel. High-quality diamond is mainly grown at high temperatures >700°C which constrains its application to materials with a high thermal budget. The ability to reduce the CVD (diamond's) growth temperature to <400°C while maintaining its excellent sp^3-like properties was crucial. At 400°C, a phase purity of ~97% was achieved which resulted in a remarkably low thermal boundary resistance of ~5 m^2K/GW with a relatively high thermal conductivity of ~300 W/m/K for a 800-nm thick layer. Furthermore, the diamond film when integrated to N-polar GaN HEMT devices measured a 70°C lower temperature in the channel at a DC power of 25 W/mm.**

INTRODUCTION

Due to the continuous need for higher performance in various applications ranging from 100's kHz (power electronics) to 100's GHz (RF electronics), GaN devices are pushed to higher power densities. This results in a higher junction temperature owing to the Joule heating in the channel resulting in device performance degradation and premature failure. As we go towards higher frequencies (W→D-band), the gain (G) becomes a premium. So, any heat removal to maintain the PAE of the device becomes critical. Heat sets a limit to P_{out} and efficiency because it triggers a vicious cycle. Heat dissipation (caused by finite PAE) causes the channel mobility to decrease which increases the knee voltage of the device (decreases drain efficiency). To break this feedback loop, removal of heat is critical, especially for devices operating at higher frequencies where G and PAE are at a premium [1]–[4]. Diamond is an excellent material that has been helpful in extracting heat, can be used to extract heat from GaN devices to reduce its channel temperature[5]-[6]. Thus far, the two methods that have been performed using synthetic diamond for thermal management of semiconductor devices are: 1) replacing the device substrate (Sapphire, SiC, or GaN) with single or polycrystalline (PC) diamond and 2) integration of PC diamond on top of the device[7]–[10]. Top-side approach can be more efficient due to the close proximity of diamond to the junction's hot spot, which makes the overall thermal resistance of the channel to the heat-sink lower. Furthermore, the top-side approach presents the potential to be more compatible with the fabrication processes since diamond can be integrated after device fabrication. The 700°C-grown diamond is suitable for integration at the material level before device fabrication for semiconductors with a higher thermal budget like GaN, Si, and SiC. The 400°C has been designed not only for integration after the device is fully fabricated but also is compatible with lower thermal budgets materials such as InP and Ga_2O_3.

RESULTS AND DISCUSSION

HIGH-TEMPERATURE DIAMOND

At Stanford (WBG-Lab), we have demonstrated thin-film diamond growth on GaN, using high-temperature (HT) growth technique at 700°C. Fig. 1a shows the plan- and cross-sectional-view SEM images of the CVD-grown diamond demonstrating more isotropic grains with similar vertical and lateral dimensions (~2 µm) compared with conventional columnar grains [11], [12]. Larger grains in the lateral direction enable phonons to travel a more extended range

before any collision with the grain boundaries. This decreased phonon scattering rate resulted in a higher in-plane thermal conductivity (TC) of 638±48 W/m/K [13].

The nucleation layer of diamond on a foreign substrate like Si_3N_4/GaN/AlGaN HEMT structure starts with diamond nanoparticles. Both the Si_3N_4 and diamond nucleation layers (ultra-nano-crystalline-diamond, UNCD) have low thermal conductivities (1.3 and <50 W/m.K, respectively). So, Si_3N_4 and the nucleation layer thicknesses were minimized for higher heat dissipation efficiencies. As shown in Fig. 1b, the nucleation layer thickness was reduced to 25-30 nm and the interfacial Si_3N_4 was thinned down to ~1 nm without imposing any structural damage to the 2DEG channel. This reduction in the thickness of the nucleation and Si_3N_4 layers along with a shallow carbon diffusion into the Si_3N_4 layer, resulted in a record low thermal boundary resistance (TBR) between the diamond and the GaN Channel as 3.1±0.7 m^2K/GW. Carbon can be diffused with a high level of controllability into the Si_3N_4 layer during the diamond growth and convert part of this layer to SiC with a relatively higher TC, as shown in Fig. 1c. The SiC formation provides a smooth atomic transform and matches phonon vibrational modes at the interface [13]. Fig. 1d summarizes the transient thermoreflectance (TTR) results of the interface TBR with different Si_3N_4 thicknesses. As expected, reducing the Si_3N_4 thickness lowered the TBR closer to diffuse-mismatch theory prediction.

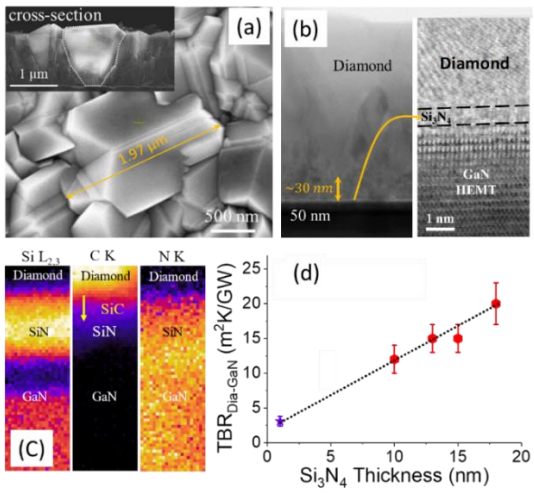

Fig. 1. a) Cross-sections and plan-view SEM images of the CVD-grown diamond on Si_3N_4/GaN/AlGaN HEMT structure. b) STEM and HRTEM micrographs of the interface confirming thin nucleation and Si_3N_4 layers. c) EELS analysis at the interface showing carbon was diffused into the Si_3N_4 and formed a thin SiC interfacial layer. d) Measured diamond-GaN TBR with respect to the Si_3N_4 thickness using TTR method.

Low-Temperature Diamond

Diamond growth at high temperatures (650-900°C), although simpler on bare materials or substrates, if grown as a thin film after the device is fully fabricated, increases gate leakage especially for high-frequency devices with thin (< 10 nm) gate dielectrics. So, in order to integrate diamond on top of fully fabricated devices and to be compatible with the BEOL process, the growth temperature must be reduced to minimize the damage. However, reducing the diamond growth temperature below 500°C without modifying the gas chemistry has been found to deteriorate the diamond phase purity, structural properties, and eventually its thermal properties [14]– [16]. We have developed a low-temperature (LT) BEOL-compatible diamond growth technique in which the addition of oxygen gas to the original gas mixture (H_2/CH_4) was necessary to preserve diamond layer quality and structural properties significantly close to that of HT-grown diamond [17].

Oxygen enhances the etching process of sp^2 by breaking one of the double bonds between carbon atoms and making it unstable. In this process, a C=C double bond is replaced by a C-C single bond. The SEM micrographs and Raman spectra of the optimized growth are shown in Fig. 2. Low magnification SEM (Fig. 2a) shows complete and uniform coverage of diamond. The high magnification SEM (Fig. 2b) realizes grains with higher crystalline level compared to the case without oxygen (inset Fig. 2a), which are extremely similar to the HT diamond growth results (Fig. 1a). As shown in Fig. 2c, the Raman spectroscopy is showing a strong diamond peak at ~1332 cm^{-1} with a narrow FWHM ~6 cm^{-1} which is another sign of high-quality LT diamond growth.

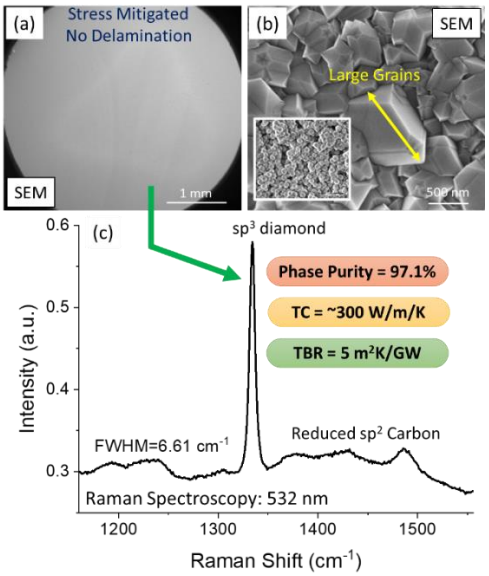

Fig. 2. a) Low magnification plan-view SEM showing no delamination and uniform diamond layer on top. b) High magnification SEM image of LT-grown diamond showing large grains and crystallite similar to HT-grown diamond. Inset figure is a plan-view SEM of diamond grown at LT without oxygen in the gas chemistry. c) Raman spectra of the LT diamond with a strong sp^3 peak ~1332 cm^{-1} and <6 cm^{-1} FWHM.

The grain size of our optimized low-temperature diamond averaged between 600-700 nm, which from theory, corresponds to an average TC between 300 and 400 W/m/K [18]. Using Transient Thermo Reflectance (TTR) method, developed at University of Bristol, and fitting the analytical model to the measured signal as shown in Fig. 3a, we have measured a TC of ~300 W/m/K, consistent with similar grain sizes grown at 700°C. The measured TC for our 400°C-diamond is approximately 200% higher than the TC reported by [19] (~110 W/m/K measured at 20°C) for 300 nm-thick nano-crystalline-diamond (NCD) film, which was grown at 450-500°C. This relatively high TC with only ~800 nm of thickness is dedicated to the near-isotropic shape of the grains which decreases the phonon scattering rate in these grains and eventually enhances its thermal properties. Another advantage of this LT diamond is the high-quality nucleation at the interface which resulted in a TBR as low as 5 m^2K/GW. This TBR is extremely close to 3.1 m^2K/GW for 700°C-grown diamond. Figure 5(b) shows EELS mapping of carbon atoms with the change in the chemical bonding at the interface. An extremely sharp transition to sp^3 carbon from the interface (point 4→3) can be observed, verifying a thin interfacial layer (less temperature profile discontinuity) and high-quality nucleation, which maintains our low TBR.

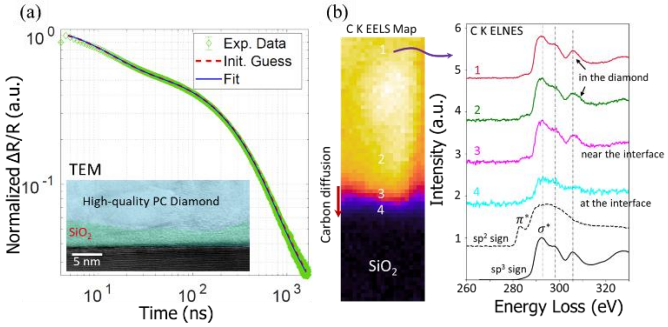

Fig. 3. (a) Normalized thermoreflectance signal as a function of time; lines represent the experimental value, and dots represent an analytical model fitted to the experimental values. (b) EELS analysis at the interface shows chemical bonding types at various points.

DEVICE-LEVEL COOLING

With all the progress achieved in diamond growth on GaN and particularly at low thermal budget, we were able to fabricate Nitrogen polar GaN HEMTs demonstrating the diamond integration process [5], [20]. The HEMTs featured a novel all-around diamond growth that was wrapped around the active region of the device and tied to the SiC substrate.

In I-V thermometry method, DC current at room temperature and pulsed current at different ambient temperatures were compared to calculate the average channel temperature along the channel between the source and drain for a given DC power [21]. As shown in Fig. 4a, the average channel temperature was recorded to be highest for the reference (w/o diamond) sample and is the lowest for the sample with a 500 nm *all-around* diamond. The all-around diamond was very efficient in spreading the heat away from the channel and then then drive it to the substrate, thus bypassing the vertical heat path through buffer layers.

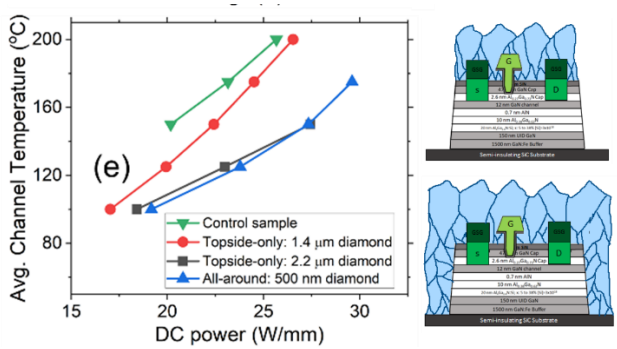

Fig. 4. The comparison of average temperature along the channel vs DC power. Improved cooling was observed with increase in the thickness of diamond in case of topside-only and in all-around case, even with a thinner diamond of 500 nm, the channel temperature was the lowest.

In addition to the IV thermometry, a thermo-reflectance system (Microsanj) was used to image the temperature profile along the gate electrode. As shown in Fig. 5a, the reference sample exhibited localized hot spots at ~17 W/mm with a maximum temperature of ~250 °C. While the sample with an all-around diamond has no localized hot spots on the gate electrode even at higher power level of 18.4 W/mm, and the temperature profile is distributed along the gate more uniformly.

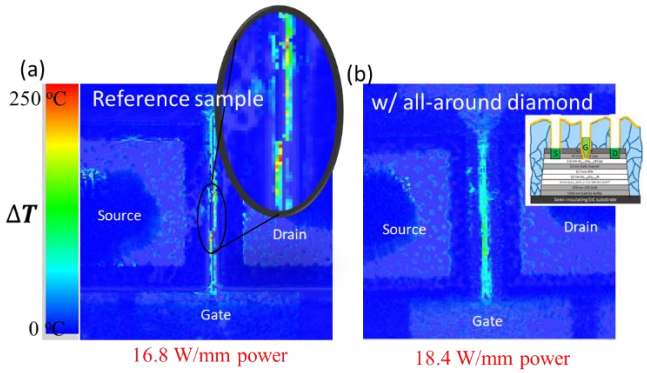

Fig. 5. Thermo-reflectance image of (a) control sample without diamond at 16.8 W/mm, and (b) all-around diamond integrated sample 18.4 W/mm DC power. Reference sample exhibited peak temperature near 250 °C with thermal hotspots. Whereas the temperature profile in all-around diamond integration sample is more uniform with less hotspots even at higher power dissipation.

We also performed and reported the use of gate resistance (R_G) technique to estimate the average temperature in the channel under the gate electrode [20]. An increase in the R_G of 9.19 Ω with ~10 W/mm power dissipation was measured

on the reference device. The R_G increased only by 3.95 Ω with ~18 W/mm power for the all-around diamond sample. As shown in Fig. 6, sample with all-around diamond exhibited a 98 ± 19 °C (measured on multiple devices over the wafer) lower temperature at the gate electrode compared to the reference sample at 9.5 W/mm DC power.

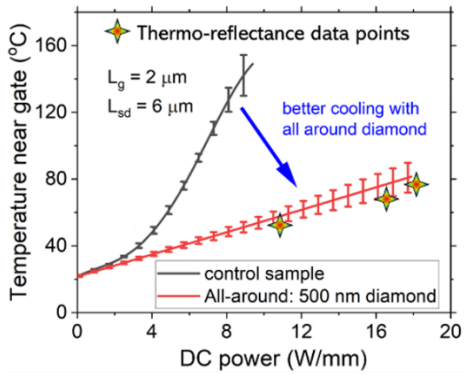

Fig. 6. Gate resistance measurement results showing much lower temperature in the channel of the sample with all-around diamond.

Conclusions

This paper presents the recent results of Diamond and GaN integration highlighting a low thermal budget process suitable for post-fabrication integration. Channel cooling was experimentally demonstrated using IV-Thermometry, Thermal imaging and Gate resistance methods and showed remarkable efficacy. Diamond integration technology looks extremely promising for the delivery of high-power density GaN devices for both power and RF electronics.

Acknowledgements

This invited paper is based on our recent achievements reported in diamond on GaN. We would like to thank all the contributors in particular R. Soman at from Stanford, and E. Akso from UCSB for their contributions to the original reports. The Diamond growth and integration was done at Stanford and was funded partly by SRC, DARPA-DSSP. At the University of Bristol TTR measurements were performed and the work was supported by DOE EFRC (ULTRA). We would like to thank Dr. Thomas Kazior and his team at DARPA, for valuable discussions.

References

[1] B. Romanczyk *et al.*, *IEEE Electron Device Letters*, vol. 41, no. 3, pp. 349–352, 2020.
[2] B. Romanczyk *et al.*, *IEEE Electron Device Letters*, vol. 41, no. 11, pp. 1633–1636, 2020.
[3] C. Prasad, S. Ramey, and L. Jiang, *IEEE International Reliability Physics Symposium Proceedings*, pp. 6A4.1-6A4.7, 2017.
[4] C. Prasad, *IEEE Trans Electron Devices*, vol. 66, no. 11, pp. 4546–4555, 2019.
[5] M. Malakoutian *et al.*, *2021 IEEE 8th Workshop on Wide Bandgap Power Devices and Applications, WiPDA 2021 - Proceedings*, pp. 70–74, 2021.
[6] T. Liu, D. Raabe, W. Mao, and S. Zaefferer, *Adv Funct Mater*, vol. 19, no. 24, pp. 3880–3891, 2009.
[7] G. H. Jessen *et al.*, *2006 IEEE Compound Semiconductor Integrated Circuit Symposium*, 2006, pp. 271–274.
[8] D. C. Dumka *et al.*, *2013 IEEE Compound Semiconductor Integrated Circuit Symposium*, 2013, pp. 1–4.
[9] M. Alomari *et al.*, *Diam Relat Mater*, vol. 20, no. 4, pp. 604–608, 2011.
[10] Y. Zhou *et al.*, *Appl Phys Lett*, vol. 111, no. 4, p. 041901, 2017.
[11] A. Sood *et al.*, *J Appl Phys*, vol. 119, no. 17, 2016.
[12] M. Malakoutian, C. Ren, K. Woo, H. Li, and S. Chowdhury, *Cryst Growth Des*, vol. 21, no. 5, pp. 2624–2632, 2021.
[13] M. Malakoutian *et al.*, *ACS Appl Mater Interfaces*, vol. 13, no. 50, pp. 60553–60560, 2021.
[14] Y. Muranaka, H. Yamashita, and H. Miyadera, *J Appl Phys*, vol. 69, no. 12, pp. 8145–8153, 1991.
[15] J. Stiegler, T. Lang, M. Nygård-Ferguson, Y. von Kaenel, and E. Blank, *Diam Relat Mater*, vol. 5, no. 3–5, pp. 226–230, 1996.
[16] X. Xiao, J. Birrell, J. E. Gerbi, O. Auciello, and J. A. Carlisle, *J Appl Phys*, vol. 96, no. 4, pp. 2232–2239, 2004.
[17] M. Malakoutian *et al.*, *Adv Funct Mater*, vol. 32, p. 2208997, 2022.
[18] J. Anaya *et al.*, *Acta Mater*, vol. 103, pp. 141–152, 2016.
[19] V. Goyal, A. v. Sumant, D. Teweldebrhan, and A. A. Balandin, *Adv Funct Mater*, vol. 22, no. 7, pp. 1525–1530, 2012.
[20] R. Soman *et al.*, *IEEE International Electron Devices Meeting*, pp. 30.8.1-30.8.4, 2023.
[21] Z. Xu *et al.*, *IEEE Transactions on Electron Devices*, vol. 65, no. 12, pp. 5301–5306, 2018.

Acronyms

PC diamond: Polycrystalline diamond
TC: Thermal Conductivity
TBR: Thermal Boundary Resistance
R_G: Gate Resistance
GaN: Gallium Nitride
WBG: Wide Band Gap
HT: High Temperature
LT: Low Temperature
UNCD: Ultra Nano Crystalline Diamond
NCD: Nano Crystalline Diamond